Duncan, R. A., Backman, J., Peterson, L. C., et al., 1990
Proceedings of the Ocean Drilling Program, Scientific Results, Vol. 115

26. CARBONATE ACCUMULATION IN THE INDIAN OCEAN DURING THE PLIOCENE: EVIDENCE FOR A CHANGE IN PRODUCTIVITY AND PRESERVATION AT ABOUT 2.4 Ma[1]

William B. Curry,[2] James L. Cullen,[3] and Jan Backman[4]

ABSTRACT

We measured carbonate concentrations in Pleistocene and Pliocene sediments deposited at Sites 709, 710, and 711. Carbonate concentrations exhibit low-amplitude, long-wave length (300–400 k.y. period) variations at the shallowest sites (709 and 710). Before 2.47 Ma, all three sites exhibit higher frequency (100 k.y. period) variations. The deepest site (711) exhibited low-amplitude variations and very low concentrations up to the Gauss/Matuyama magnetic reversal (2.47 Ma), then concentrations abruptly increased. After 2.47 Ma, carbonate concentrations at Site 711 exhibited the same periodic changes as at Site 709. Although a long wave-length periodicity (260–280 k.y.) occurs at these sites after 2.47 Ma, the 100 k.y. period is absent. The dominant periods observed in these data are those found in the eccentricity component of the earth's orbital geometry.

Estimates of carbonate accumulation at Sites 709 and 710 document that surface-water productivity decreased near the Gauss/Matuyama magnetic reversal whereas accumulation at Site 711 increased. These results indicate that the rate of carbonate preservation in the deep Indian Ocean increased at that time. This increase in preservation may have resulted from a decrease in the production rate of carbonate in tropical oceans of the world. Carbonate accumulation estimated from sediments in shallow locations (~3000–3800 m) of the Atlantic and Pacific oceans also indicates that carbonate production decreased at this time. A consequence of lowered surface-water productivity is increased carbonate ion concentration of the deep ocean and better preservation of carbonate on the seafloor.

INTRODUCTION

One of the principal goals of Ocean Drilling Program (ODP) Leg 115 was to reconstruct the history of carbonate sedimentation in the western Indian Ocean during the Neogene. The drilling strategy, to core a series of holes down the northern slope of the Madingley Rise, produced a series of three sites (709, 710, and 711) that span the water depth interval from 3000 to 4400 m. We have measured the carbonate concentration of the Pliocene sediments that spanned the interval associated with the most recent phase of Northern Hemisphere ice growth (~2.4 Ma). The purpose of our study is to determine what changes in the carbonate system occurred in response to this major change in the earth's climate.

Our research strategy is based on studies of late Quaternary sedimentation and sediment geochemistry that have successfully reconstructed many aspects of late Quaternary deep-water circulation and chemistry (Johnson et al., 1977; Curry and Lohmann, 1983, 1985, in press; Peterson and Prell, 1985a). This strategy invokes a basic assumption that the principal source of carbonate in the sediments at this location is from surface-water productivity, with little or no lateral input from advection or down-slope reworking. If this assumption is true, then carbonate accumulation in the shallowest sites, if they are always above the lysocline, is the best approximation of the past history of surface-water carbonate productivity. If the sites are located close to one another and not near any sharp gradients in surface-water productivity, then the input rate of carbonate from surface water should be nearly equal in all sites. Then the difference in accumulation between the shallowest and progressively deeper sites is a quantitative estimate of the amount of carbonate lost to dissolution. Thus, our research strategy constrains the history of two important components of the carbonate system: carbonate productivity and dissolution.

METHODS

We employed a new, automated system to measure the carbonate concentration of the sediments. The system determines the carbonate concentration based on the amount of gas evolved during the chemical reaction of a known mass of dried sediment (0.01–0.02 g) in 100% phosphoric acid at a constant temperature of 80°C. The pressure of the evolved gas is converted to mass of carbonate based on the regression line of pressure vs. mass of carbonate determined for pure carbonate samples reacted in the same system. Thus, the fraction of carbonate equals the ratio of the mass of carbonate estimated from this regression and the mass of raw sediment. The system is microprocessor controlled and interfaced with a digital balance (Ostermann et al., 1990), so that the only manual operations include placing the sediment samples into the reaction boats and loading the boats into the system. Based on three sets of replicate analyses of marine sediment samples, the precision of these measurements ranges from ±0.5% to 0.8% (Fig. 1). We analyzed samples at 10-cm spacing in Site 709 and at 5-cm spacing in Sites 710 and 711 for a total of 1097 analyses. The carbonate concentration data are presented in the Appendix.

RESULTS

Site 709

Two holes at this site (3°55′S, 60°33′E, 3038 m water depth) were cored with the advanced piston corer (APC) to a depth of about 200 m. We analyzed the section from about 3 m below seafloor (mbsf) to 37 mbsf in Hole 709B (Fig. 2). The carbonate concentration throughout this interval is fairly constant with an average value of 91.3% ± 2.1% (N = 335). These values are typical of shallow cores in this region (e.g., RC12-328) and result from a low input rate of noncarbonate, terrigenous sedimentary components and a low dissolution rate. All of the car-

[1] Duncan, R. A., Backman, J., Peterson, L. C., et al., 1990. *Proc. ODP, Sci. Results*, 115: College Station, TX (Ocean Drilling Program).

[2] Department of Geology and Geophysics, Woods Hole Oceanographic Institution, Woods Hole, MA, 02543, U.S.A.
[3] Department of Geological Science, Salem State College, Salem, MA 01945, U.S.A.
[4] Department of Geology, University of Stockholm, Stockholm, Sweden.

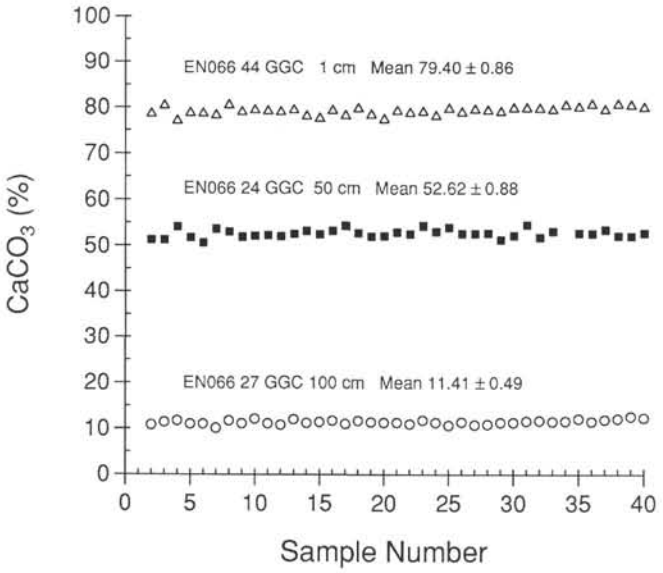

Figure 1. Replicate analyses of carbonate concentration for samples with high, medium, and low concentrations. The sediments are from Giant Gravity Cores (GGC) recovered during cruise *Endeavor* 066 (EN066) to the Sierra Leone Rise in the eastern equatorial Atlantic (Curry and Lohmann, 1985). The data were produced using an automated, digital, gasometric system with a precision of ±0.5%–0.8% (Ostermann et al., 1990).

bonate concentrations fall between 86% and 97%. Within this hole, seven magnetic reversals were identified (Schneider and Kent, this volume). We used four of these reversals to produce the time series of carbonate concentration.

Site 710

Two holes at this site (4°19′S, 60°59′E, 3812 m water depth) were cored with the APC. In Hole 710A we analyzed samples from Cores 115-710A-3H and -4H, and in Hole 710B we analyzed samples from Cores 115-710B-4H and -5H (Fig. 3). Carbonate concentrations in Hole 710A average 72.7% ± 6.7% (N = 276) and in Hole 710B they average 71.4% ± 7.1% (N = 201). Carbonate concentrations exhibit greater variability in these holes than in Hole 709B. Minimum concentrations are generally 60% whereas maximum concentrations exceed 80%. Magnetic reversals in these holes were used to produce a time series of carbonate concentration from ~5 Ma to ~2.3 Ma with a 200,000 yr gap at about 3 Ma.

Site 711

This site lies between the Madingley Rise and the Carlsberg Ridge (2°45′S, 61°10′E, 4430-m water depth). Two holes were drilled at Site 711, and we measured the carbonate concentration in Cores 115-711A-2H and -3H for Hole 711A and in Core 115-711B-3H for Hole 711B (Fig. 4). Carbonate concentrations average 27.5% ± 17.9% (N = 135) in Hole 711A and 6.3% ± 7.9% (N = 150) in Hole 711B. Overall, the average carbonate concentration is 16.3% ± 17.2% (N = 285). In the deeper sections of these holes, very low carbonate concentrations were observed. At about 14 mbsf in Hole 711A, the carbonate concentration abruptly increases to values that are consistently greater than about 25%. Maximum values at about 9 mbsf reach 75%. Magnetic reversals in these cores were identified (Schneider and Kent, this volume), and we have used these reversals to combine

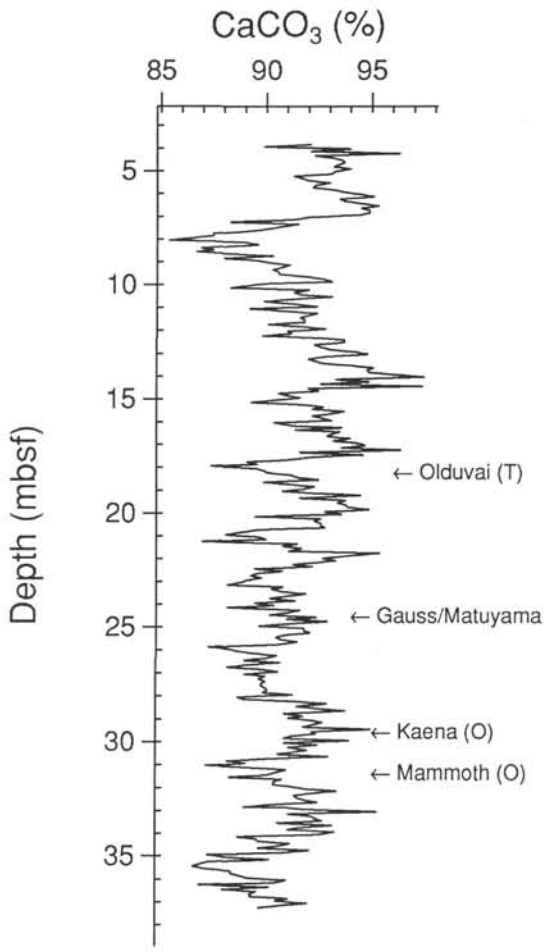

Figure 2. Carbonate concentrations in Hole 709B. Carbonate percentages average 91.3% ± 2.1% in this hole. The four magnetic reversal boundaries (Schneider and Kent, this volume) identified in the figure were used to produce the time series of carbonate concentration presented in Figure 5.

the records to produce a continuous time series of carbonate concentration for this site for the interval from ~5 to ~1.4 Ma.

Carbonate Concentration Time Series

Time series of carbonate concentration are plotted in Figure 5. Throughout the last 4 m.y., the carbonate concentration in Hole 709B does not exhibit any abrupt changes. The changes in concentration appear periodic with a long wave length (~400,000 yr). In Site 710, the combined record includes intervals with very high-frequency changes in carbonate concentration. The combined record for Site 711 exhibits some very sharp changes in carbonate concentration that correlate with major events in the Pliocene isotopic record (Shackleton et al., 1984; Keigwin, 1986). At about 2.8 Ma, carbonate concentration increases from values near 0 to values that average 10%–20%. At about 2.4 Ma, the carbonate concentration increases again to values that average >30%. The increase is very abrupt and, since the event at 2.4 Ma occurs entirely within Hole 711A, it is not a result of combining the records from Holes 711A and 711B. This increase in concentration correlates with a major increase in $\delta^{18}O$ observed above the Gauss/Matuyama magnetic reversal in many APC sites where Pliocene sediments have been recovered (Shack-

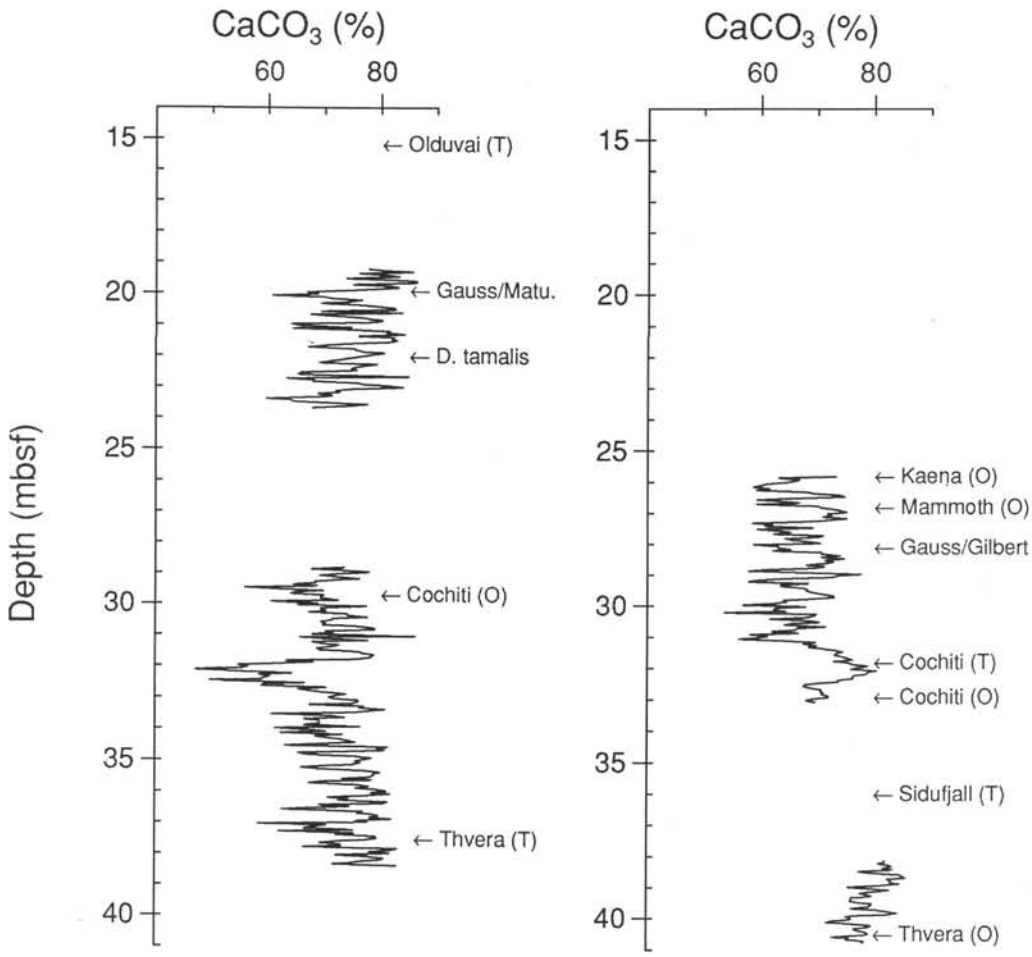

Figure 3. Carbonate concentrations in Holes 710A (left) and 710B (right). Carbonate percentages average 72.7% ± 6.7% in Hole 710A and 71.4% ± 7.1% in Hole 710B. The identified magnetic reversals (Schneider and Kent, this volume) and one biostratigraphic boundary were used to combine the data sets and to produce the time-series record for Site 710, which is presented in Figure 5.

leton et al., 1984; Keigwin, 1986). The earlier increase in concentration at 2.8 Ma correlates with isotopic events that predate the increase at 2.4 Ma (Keigwin, 1986).

A low-frequency, periodic signal is apparent in the carbonate concentration record of Site 709. Decomposing this signal into its spectral components (Fig. 6) reveals high-amplitude variations at about a 400-k.y. period (frequency = 0.0025 cycles/k.y.) during the interval from 2.47 to 3.40 Ma. After 2.47 Ma, the most prominent period in the carbonate concentration record is about 267 k.y. (frequency = 0.0037 cycles/k.y.). These same periodic changes are apparent in sections of Sites 710 and 711. Before the Gauss/Matuyama magnetic reversal, carbonate concentrations in Site 710 varied with a period of 333,000–400,000 yr. Following the Gauss/Matuyama magnetic reversal, carbonate concentrations in Site 711 varied with a period of about 285 k.y. (In Site 710, the record is too short to resolve any low-frequency changes in carbonate concentration after 2.47 Ma. In Site 711, low carbonate concentrations of small amplitude occurred before 2.47 Ma, so the record of low-frequency variations may be obscured.) Pisias and Prell (1985) also noted low-frequency variations (period = ~300 k.y.) in carbonate concentration in the Pliocene interval of Pacific Deep Sea Drilling Project (DSDP) Site 572. Periodic variations with a wave length of about 100 k.y. occur in all three sites before 2.47 Ma, but they cannot be resolved after that time (Fig. 6).

Bulk Density and Sediment Accumulation

Shipboard measurements of dry-bulk density (dry wt/wet vol.) are plotted in Figure 7 with respect to their carbonate concentration. (Note: We used only those shipboard measurements from cores that we analyzed for carbonate concentration. Although there are many more bulk density measurements available, they are mostly from deeper sections in these holes and suffer from compaction because of sediment overburden.) The correlation coefficient between the two variables is 0.95 (N = 25). The slope and intercept are very similar to those found in other equatorial regions (equatorial Pacific: Lyle and Dymond, 1976; eastern equatorial Atlantic: Curry and Lohmann, 1985, 1986), which indicates that similar sedimentary components have mixed at this location to produce the carbonate concentrations and bulk densities. In the equatorial Pacific and eastern equatorial Atlantic, the noncarbonate component is opaline silica, which has a grain density lower than calcium carbonate and terrigenous silicates. Addition of silica to the sediment lowers the carbonate concentration as well as the bulk density. In regions with low input of opaline silica but high input of terrigenous silicates, bulk density is more constant over a wide range of carbonate concentrations (Curry and Lohmann, in press).

We used the carbonate concentration, bulk density, and sedimentation rates to calculate the accumulation rate of carbonate

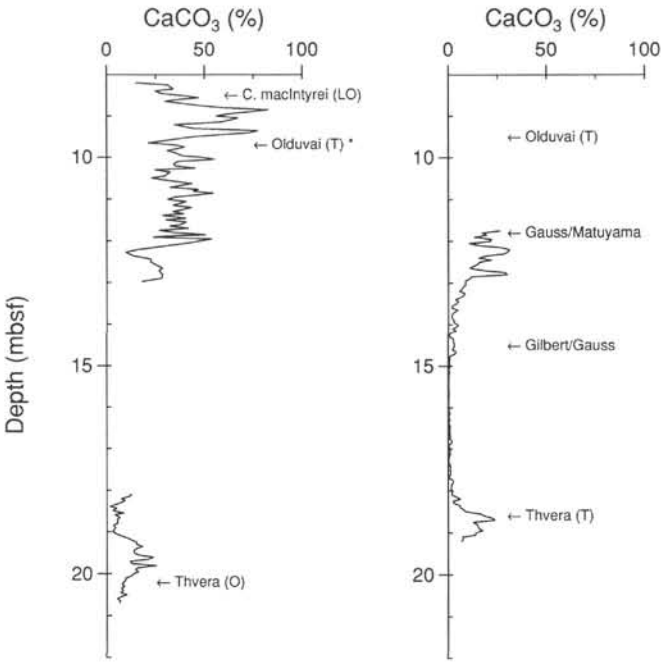

Figure 4. Carbonate concentrations in Holes 711A (left) and 711B (right). Carbonate percentages average 27.5% ± 17.9% in Hole 711A and 6.3% ± 7.9% in Hole 711B. The identified magnetic reversals (Schneider and Kent, this volume) and one biostratigraphic boundary were used to combine the records and to produce the time-series record for Site 711, which is presented in Figure 5. Note that the Olduvai (T) reversal was not identified in Hole 711A. Its level in this hole was projected from the magnetic reversal record in Hole 711B by correlating their magnetic susceptibility records.

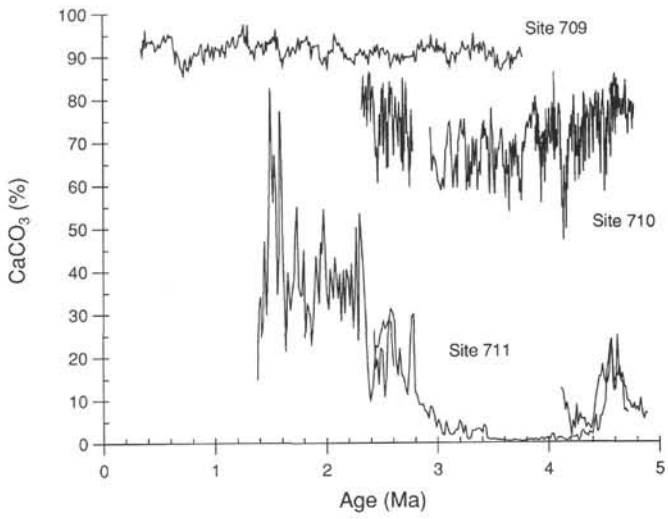

Figure 5. Time series of carbonate concentration for Sites 709, 710, and 711. The carbonate record for Site 709 exhibits low-frequency variations with a wave length of about 400 k.y. In the deepest site (711), carbonate concentrations increase at about 2.8 Ma and then very abruptly increase again at about 2.4 Ma. The abrupt increase at 2.4 Ma correlates with the $\delta^{18}O$ increase that marks the beginning of the latest phase of ice growth in the Northern Hemisphere (Shackleton et al., 1984). The earlier increase in concentration may correlate with the earlier $\delta^{18}O$ increase observed by Keigwin (1986). The chronology is not accurate enough to be certain of this correlation.

and noncarbonate sediment components for these sites so that we could evaluate the changes in productivity and preservation that affected this region during the Pliocene (Fig. 8). Average accumulation rates are presented for the intervals before and after the Gauss/Matuyama magnetic reversal (Table 1) because near this stratigraphic boundary a global increase in $\delta^{18}O$ occurred that marks the most recent phase of Northern Hemisphere ice growth (Shackleton et al., 1984; Keigwin, 1986).

Before the Gauss/Matuyama boundary, carbonate accumulation in Hole 709B averaged 0.74 g/cm^2/k.y. After this magnetic reversal, the accumulation rate decreased to 0.62 g/cm^2/k.y. This decrease in accumulation, if not accompanied by any change in dissolution at this shallow depth, must reflect a small decrease in the production of carbonate in the overlying surface water. (Note: The timing of the change in carbonate accumulation is not constrained by this data. In Figure 8, it occurs at 2.47 Ma only as an artifact because our chronology forces a change in sedimentation rate at that interval. Based on the changes in carbonate concentration at Site 711 that were caused by this decrease in carbonate productivity, we think that the decrease in carbonate accumulation may have occurred in two steps: at 2.8 Ma and 2.4 Ma.) Carbonate accumulation in Site 710 also decreased at about this time, from pre-Gauss/Matuyama values of 0.46 g/cm^2/k.y. to post-Gauss/Matuyama values of 0.36 g/cm^2/k.y. Although Site 710 is only 800 m deeper than Site 709, 0.3 g/cm^2/k.y. (about 40%) of carbonate on average have been lost to dissolution before and after the Gauss/Matuyama magnetic reversal. At Site 711 very little carbonate is accumulating either before or after the Gauss/Matuyama magnetic reversal. More than 90% of the carbonate that settled through the water column to the seafloor has subsequently dissolved. Site 711 is the only site to exhibit an increase in carbonate accumulation across the Gauss/Matuyama magnetic reversal, increasing from 0 to 0.02 g/cm^2/k.y. at 2.8 Ma and from 0.02 to 0.06 g/cm^2/k.y. at 2.4 Ma.

Noncarbonate accumulation was low in all three sites. In the shallowest hole, noncarbonate accumulation averaged 0.08 g/cm^2/k.y. before 2.47 Ma and 0.06 g/cm^2/k.y. after 2.47 Ma. In Site 710 a decrease also occurred, from values of 0.17 g/cm^2/k.y. before 2.47 Ma to 0.10 g/cm^2/k.y. after 2.47 Ma. In the deepest site, low values of 0.11 g/cm^2/k.y. occurred before and after the Gauss/Matuyama magnetic reversal. The slight bathymetric increase in noncarbonate accumulation implies that downslope reworking or advection of sediment components may have affected these sites. In a region with no lateral input of sediment, the refractory noncarbonate material should not exhibit any change in accumulation as a function of water depth (Curry and Lohmann, 1986). In these sites, noncarbonate accumulation increases slightly with depth in the water column after 2.47 Ma. Before 2.47 Ma, little difference in accumulation occurred between the shallowest and deepest site, but the middle site (710) had nearly twice the accumulation of noncarbonate material. It is difficult to evaluate the significance of these changes in noncarbonate accumulation because the values are so low in all cases. To quantify the extent of downslope or lateral input of material, it is necessary to measure the carbonate and noncarbonate accumulation rates in the smaller size fractions, as they are the sizes most likely to be affected by resuspension and redeposition (Curry and Lohmann, 1986). However, the existence of an increase in noncarbonate accumulation with depth in the water column cautions us to be concerned that carbonate may also have been transported into the deeper sites at this location by processes other than vertical settling. Therefore, our estimates of carbonate lost to dissolution should be considered "minima."

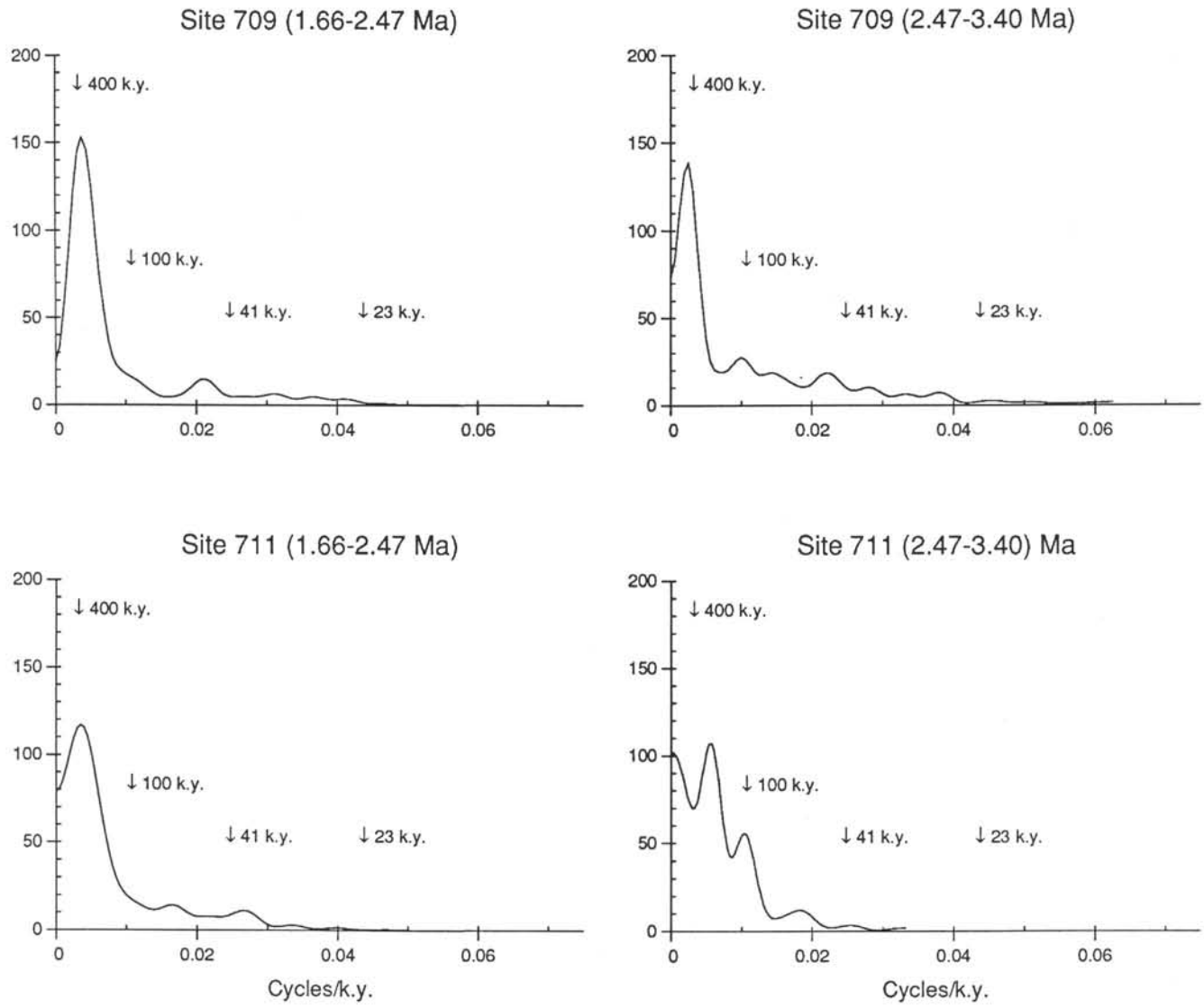

Figure 6. Spectral analysis of Sites 709 and 711. Note that most of the power in these records is concentrated at low frequency. Before 2.47 Ma, Sites 709 and 710 (not shown) each exhibit a strong 400 k.y. period and a minor 100 k.y. period. Site 711 also has power at about 100 k.y., but no power at 400 k.y. After 2.47 Ma, Sites 709 and 711 each exhibit a strong 260–280-k.y. period. No 100 k.y. period is apparent in any of the sites after 2.47 Ma.

DISCUSSION

History of Carbonate Productivity

In Site 709, the carbonate accumulation rate decreased by ~ 0.1 g/cm^2/k.y. after the Gauss/Matuyama magnetic reversal. This change in accumulation, if not caused by any change in carbonate dissolution, reflects a decrease in the production of carbonate in the overlying surface water. Dissolution changes have affected the sediments at this site (Cullen, this volume), but fortunately dissolution decreased after the magnetic reversal. Before 2.47 Ma, the ratio of foraminifer test fragments to whole tests was high, indicating that dissolution may have caused at least some loss of carbonate (Cullen, this volume). (Significant fragmentation of foraminifers can occur without measurable loss of $CaCO_3$; Peterson and Prell, 1985b.) Therefore, the carbonate accumulation measured in Hole 709B before 2.47 Ma is a minimum estimate of the carbonate productivity rate in the surface waters at that time. After 2.47 Ma, dissolution (measured as the fragmentation ratio) and carbonate accumulation decreased, so the decrease in accumulation was not caused by changes in dissolution. Thus, we are confident that a decrease in productivity occurred at about 2.47 Ma and that ~ 0.1 g/cm^2/k.y. (the difference between the pre- and post-2.47 Ma values) is a minimum estimate of the decrease.

Throughout the Pliocene, Site 710 always had a lower carbonate accumulation than Site 709 (by 0.3 g/cm^2/k.y.). Thus, dissolution must have influenced the accumulation rate of carbonate at Site 710. Its carbonate accumulation also decreased by ~ 0.1 g/cm^2/k.y. after the Gauss/Matuyama magnetic reversal, the same difference observed in Site 709. This decrease in accumulation may have resulted from the same decrease in surface-water productivity implied by the record of Site 709, but unfortunately our conclusion is ambiguous for two reasons. First, we have less confidence in our mean value for the 1.66–2.47-Ma interval because we sampled only a small number of sediments from just above the Gauss/Matuyama magnetic reversal. Second, we have no independent control over the changes in dissolution at this depth. We think that the dissolution rate

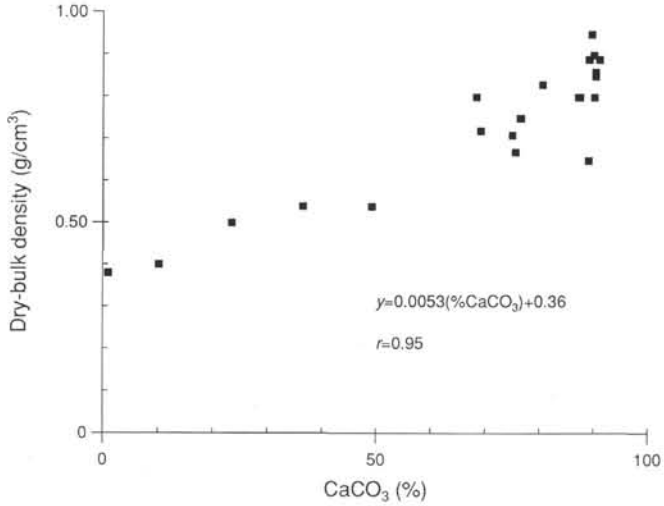

Figure 7. Dry-bulk density and carbonate concentration from shipboard measurements that were performed during Leg 115. The relationship between carbonate concentration and dry-bulk density is similar to the relationships that are observed in other equatorial locations where biogenic opal is the principal noncarbonate component of the sediment (Lyle and Dymond, 1976; Curry and Lohmann, 1985). Based on this strong correlation, we have used the carbonate concentration data to predict sediment bulk density in all of our accumulation rate calculations.

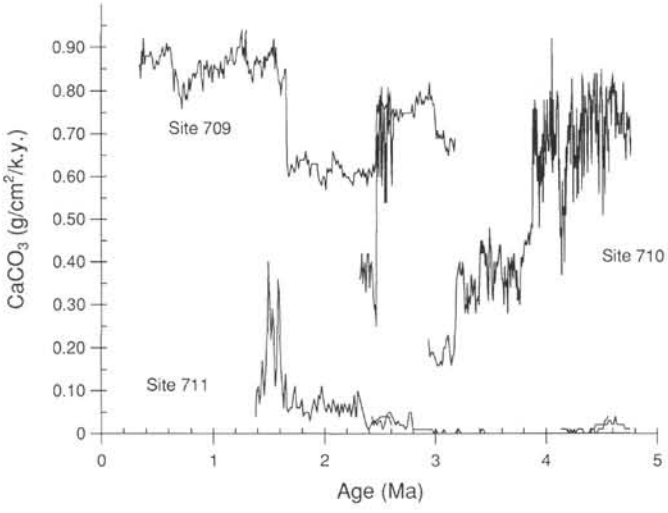

Figure 8. Carbonate accumulation rate variations for Sites 709, 710, and 711. Carbonate accumulation in Site 709 decreased on average by about 0.1 g/cm^2/k.y. at the Gauss/Matuyama magnetic reversal (2.47 Ma). At the same time, accumulation in the deepest site (711) increased. This pattern of carbonate accumulation implies that, in the Indian Ocean, carbonate productivity decreased at 2.47 Ma while dissolution on the seafloor decreased. Parallel decreases in carbonate accumulation in Pliocene sediments of the Atlantic and Pacific oceans suggest that carbonate productivity may have decreased in many tropical locations at this time. A mean decrease in carbonate productivity, if it is not accompanied by a change in river input of Ca and CO_3, would decrease the corrosiveness of deep water and increase carbonate preservation on the seafloor.

Table 1. Calculated accumulation rates of $CaCO_3$ and non-$CaCO_3$ for Sites 709, 710, and 711.

	1.66–2.47 Ma			2.47–3.40 Ma		
Site	$CaCO_3$	non-$CaCO_3$	#	$CaCO_3$	non-$CaCO_3$	#
709	0.62 ± 0.02	0.06 ± 0.01	N = 63	0.74 ± 0.04	0.08 ± 0.01	N = 68
710	0.36 ± 0.05	0.10 ± 0.03	N = 18	0.46 ± 0.22	0.17 ± 0.06	N = 87
711	0.06 ± 0.02	0.11 ± 0.01	N = 53	0.02 ± 0.02	0.11 ± 0.01	N = 62

Note: The data are presented as averages (in g/cm^2/k.y.) for the intervals between the Oldavai (T) and the Gauss/Matuyama magnetic reversals (1.66–2.47 Ma) and the Gauss/Matuyama and Gauss/Gilbert (2.47–3.40 Ma) magnetic reversals.

did not increase since dissolution decreased in Site 709 (Cullen, this volume) and because we observe an increase in preservation in deeper Site 711.

History of Carbonate Dissolution

Of the three sites, only Site 711 experienced an increase in carbonate accumulation after the Gauss/Matuyama magnetic reversal. Although the increase is small, it is significant ($p < 0.005$) because of the large number of analyses that have been used to produce the mean values. Because the accumulation rate in the two shallower sites decreased after the magnetic reversal, Site 711 also probably experienced a decreased input rate of carbonate because of lower surface-water productivity after 2.47 Ma. Thus, the increase in carbonate accumulation in Site 711 after 2.47 Ma must have resulted from an increase in the preservation of calcium carbonate. (Changes in advection or downslope reworking of carbonate are not likely the cause of the increase in carbonate accumulation because the accumulation rate of the insoluble fraction in Site 711 is the same before and after 2.47 Ma.)

Carbonate preservation in the deep sea is controlled by processes that may act on the ocean as a whole (e.g., changes in surface-water productivity) or locally (changes in the location, chemistry, or production rate of deep water). To determine the cause of this change in preservation in Site 711, we must compare the changes in carbonate sedimentation at this location to those observed in the tropical Pacific and Atlantic oceans. For the Pacific, carbonate concentration data of comparable temporal resolution and shallow depth are available from Site 503 (4°3′N, 95°38′W, 3672 m water depth), and for the Atlantic (Caribbean), data are available from Site 502 (11°29′N, 79°23′W, 3051-m water depth). We used the carbonate data from these sites (Prell, Gardner, et al., 1982) to determine if there were global changes in carbonate accumulation that may be related to changes in carbonate production.

Table 2 summarizes the changes in carbonate accumulation in the Atlantic (Site 502) and Pacific (Site 503) oceans that occurred at the Gauss/Matuyama magnetic reversal. Carbonate accumulation decreased in both sites at this time. In the Atlantic location, carbonate accumulation decreased from pre-2.47 Ma values of 1.76 g/cm^2/k.y. to post-2.47 Ma values of 1.66 g/cm^2/k.y. In the Pacific Ocean location, carbonate accumulation decreased from 0.59 to 0.53 g/cm^2/k.y. These decreases in accumulation occur at water depths that are above the present depth of the carbonate lysocline. The decreases in accumulation observed in Sites 502 and 503 are on the same order (~0.1 g/cm^2/k.y.) as the decrease observed in Site 709. Taken together, these data imply that the production rate of carbonate in the surface waters of tropical locations decreased near the Gauss/Matuyama magnetic reversal, in response to the cooling associated with Northern Hemisphere ice growth. Although the decrease in average productivity rate is clearly evident, the exact timing of the decrease is unconstrained by these data; our accumulation rates are forced to change at the magnetic reversal because the

Table 2. Calculated accumulation rates of $CaCO_3$ for Sites 502 (Atlantic) and 503 (Pacific).

Site	1.66–2.47 Ma	2.47–3.40 Ma
502	1.66	1.76
503	0.53	0.59

Note: The carbonate data used in the calculations are from Prell, Gardner, et al. (1982). The data are presented as averages (in $g/cm^2/k.y.$) for the intervals between the Olduvai (T) and Gauss/Matuyama magnetic reversals (1.66–2.47 Ma) and the Gauss/Matuyama and Gauss/Gilbert (2.47–3.40 Ma) magnetic reversals.

reversal provides our sedimentation rate constraint. But on the basis of the effect of the decrease on carbonate productivity on preservation at the deepest site, we think that productivity may have changed in two steps, one at 2.8 Ma and one at 2.4 Ma.

The increases in carbonate accumulation observed at this time in the deepest Indian Ocean site (711) most likely resulted from a decrease in carbonate productivity of the tropical oceans. In today's ocean, carbonate productivity far exceeds the rate of carbonate burial that is needed to balance the river input of calcium and carbonate. Consequently, only about a third of the carbonate produced in surface water survives chemical destruction on the shallow flanks of submarine rises and ridges. If the rate of productivity decreased without any net change in river input, the lysocline and carbonate compensation depth (CCD) must migrate to deeper locations if the balance of carbonate and calcium in the deep ocean is to be maintained. We think that the evidence presented here supports our hypothesis to explain the pattern of carbonate accumulation in Site 709, 710, and 711: a decrease in carbonate productivity of surface waters lowered the demand for carbonate dissolution needed to balance river input. Consequently, the dissolution rate decreased in Site 711, which in turn increased its carbonate concentration and carbonate accumulation rate.

CONCLUSIONS

Carbonate sedimentation patterns changed near the Gauss/Matuyama magnetic reversal in response to the major change in the earth's climate at that time. Based on these changing patterns, we conclude:

1. Surface-water productivity of carbonate-producing organisms decreased by about 0.1 $g/cm^2/k.y.$ in the western tropical Indian Ocean. Based on data from shallow APC sites in the tropical Atlantic and Pacific oceans, carbonate accumulation also decreased. If these sites were shallower than the carbonate lysocline at that time, then the evidence indicates that carbonate productivity may have decreased in all tropical regions of the oceans.

2. Dissolution decreased in the deepest parts of the western Indian Ocean, which caused increased carbonate concentration and accumulation in Site 711 after the Gauss/Matuyama magnetic reversal. This decrease in dissolution may have been a consequence of a decrease in carbonate productivity in the tropical Atlantic, Indian, and Pacific oceans.

3. Before 2.47 Ma, low-frequency variations with a period of 400 k.y. dominated the records of carbonate concentration. After 2.47, the low-frequency periodic component was closer to 280 k.y. in duration. Before 2.47 Ma, all sites exhibit variations in carbonate concentrations with a wave length of about 100 k.y. These wave lengths are characteristic of eccentricity variations in the earth's orbit, implying that orbital variations affected the carbonate system during the early Pliocene.

ACKNOWLEDGMENTS

The carbonate data presented in this paper were produced by D. R. Ostermann. This paper benefited from reviews by two anonymous reviewers. We thank them for many useful comments. Although not supported by a specific grant, the research strategy used in this paper was developed through grants from the National Science Foundation. This is Woods Hole Oceanographic Institution Contribution No. 7397.

REFERENCES

Curry, W. B., and Lohmann, G. P., 1983. Reduced advection into Atlantic Ocean deep eastern basins during last glaciation maximum. *Nature*, 306:577–580.

_____, 1985. Carbon deposition rates and deep water residence time in the equatorial Atlantic Ocean throughout the last 160,000 years. *In* Sundquist, E. T., and Broecker, W. S. (Ed.), *The Carbon Cycle and Atmospheric CO_2: Natural Variations Archean to Present*. Am. Geophys. Union Monogr., 32:285–301.

_____, 1986. Late Quaternary carbonate sedimentation at the Sierra Leone Rise (eastern equatorial Atlantic Ocean). *Mar. Geol.*, 70:223–250.

_____, in press. Reconstructing past particle fluxes in the tropical Atlantic Ocean. *Paleoceanography.*

Johnson, D. A., Ledbetter, M., and Burckle, L. H., 1977. Vema Channel paleo-oceanography: Pleistocene dissolution cycles and episodic bottom water flow. *Mar. Geol.*, 23:1–33.

Keigwin, L. D., 1986. Pliocene stable-isotope record of Deep Sea Drilling Project Site 606: sequential events of ^{18}O enrichment beginning at 3.1 Ma. *In* Ruddiman, W. F., Kidd, R. B., Thomas, E., et al., *Init. Repts. DSDP*, 94, Pt. 2: Washington (U.S. Govt. Printing Office), 911–920.

Lyle, M. W., and Dymond, J., 1976. Metal accumulation rates in the southeast Pacific—errors introduced from assumed bulk densities. *Earth Planet. Sci. Lett.*, 30:164–168.

Ostermann, D. R., Karbott, D., and Curry, W. B., 1990. Automated system to measure the carbonate concentration of sediments. Woods Hole Oceanogr. Inst. Tech. Rep. WHOI-90-03.

Peterson, L. C., and Prell, W. L., 1985a. Carbonate preservation and rates of climatic change: an 800 kyr record from the Indian Ocean. *In* Sundquist, E. T., and Broecker, W. S. (Ed.), *The Carbon Cycle and Atmospheric CO_2: Natural Variations Archean to Present*. Am. Geophys. Union Monogr., 32:251–269.

_____, 1985b. Carbonate dissolution in Recent sediments of the eastern equatorial Indian Ocean: preservation patterns and carbonate loss above the lysocline. *Mar. Geol.*, 64:259–290.

Pisias, N. G., and Prell, W. L., 1985. High resolution carbonate records from the hydraulic piston cored section of Site 572. *In* Mayer, L., Theyer, F., Thomas, E., et al., *Init. Repts. DSDP*, 85: Washington (U.S. Govt. Printing Office), 711–722.

Prell, W. L., Gardner, J. V., et al., 1982. *Init. Repts. DSDP*, 68: Washington (U.S. Govt. Printing Office).

Shackleton, N. J., Backman, J., Zimmerman, H. B., Kent, D. V., Hall, M. A., Roberts, D. G., Schnitker, D., Baldauf, J. G., Desprairies, A., Homrighausen, R., Huddleston, P., Keene, J. B., Kaltenback, A. J., Krumsiek, K.A.O. Morton, A.C., Murray, J. W., and Westberg-Smith, J., 1984. Oxygen isotope calibration of the onset of icerafting in DSDP Site 552A: history of glaciation in the North Atlantic region. *Nature*, 307:620–623.

Date of initial receipt: 11 September 1989
Date of acceptance: 22 January 1990
Ms 115B-164

APPENDIX

Carbonate Concentrations for Sites 709, 710, and 711.

Depth (msbf)	Age (Ma)	$CaCO_3$ (%)
115-709B-2H-		
3.84	0.345	92.1
3.94	0.354	89.9
4.04	0.363	94.0
4.14	0.371	92.1
4.24	0.380	96.3
4.34	0.389	92.3
4.44	0.398	93.2
4.54	0.407	93.6
4.64	0.416	93.7
4.74	0.425	93.4
4.83	0.433	93.2
4.92	0.441	94.0
5.04	0.452	93.2
5.14	0.461	93.1
5.24	0.470	91.3
5.34	0.479	91.7
5.44	0.488	92.0
5.54	0.497	93.0
5.64	0.506	92.3
5.74	0.515	92.2
5.84	0.524	93.2
5.94	0.533	93.7
6.03	0.541	94.4
6.14	0.551	95.1
6.24	0.560	93.5
6.33	0.568	93.7
6.42	0.576	94.4
6.54	0.587	95.3
6.64	0.596	94.5
6.74	0.605	94.9
6.84	0.614	94.9
6.94	0.623	94.4
7.04	0.632	92.0
7.14	0.641	91.3
7.24	0.650	88.3
7.34	0.659	91.5
7.44	0.668	90.7
7.54	0.677	90.1
7.64	0.686	89.2
7.74	0.695	87.5
7.84	0.703	87.5
7.95	0.713	86.4
8.04	0.721	85.4
8.12	0.729	88.9
8.24	0.739	89.6
8.38	0.752	86.9
8.46	0.759	87.5
8.55	0.767	86.7
8.64	0.775	88.3
8.74	0.784	90.3
8.84	0.793	88.0
8.94	0.802	89.6
9.04	0.811	90.2
9.14	0.820	91.1
9.25	0.830	90.7
9.35	0.839	90.3
9.46	0.849	90.6
9.55	0.857	90.6
9.66	0.867	91.9
9.76	0.876	92.7
9.88	0.887	93.1
9.96	0.894	90.0
10.05	0.902	89.1
10.14	0.910	88.3
10.24	0.919	92.0
10.35	0.929	91.3
10.44	0.937	91.6
10.54	0.946	93.1
10.64	0.955	91.3
10.74	0.964	89.9
10.86	0.974	91.4
10.97	0.984	92.4
11.05	0.992	89.2
11.16	1.001	90.9
11.26	1.010	92.4
11.44	1.027	91.6
11.54	1.035	91.8
11.64	1.044	91.8
11.74	1.053	90.1
11.84	1.062	91.7
11.94	1.071	92.8
12.04	1.080	91.0
12.14	1.089	91.2
12.24	1.098	89.8
12.34	1.107	92.5
12.42	1.114	93.7
12.53	1.124	93.7
12.63	1.133	92.3
12.73	1.142	92.6
12.84	1.152	93.1
12.94	1.161	94.3
13.04	1.170	94.8
13.14	1.179	92.8
13.25	1.189	92.0
13.33	1.196	92.3
13.44	1.206	92.7
13.54	1.215	94.1
13.64	1.224	95.1
13.74	1.233	94.8
13.84	1.242	94.9
13.94	1.251	96.1
14.04	1.260	97.5
14.14	1.269	93.3
14.24	1.278	94.9
14.34	1.287	92.6
14.44	1.296	97.4
14.53	1.304	92.0
14.65	1.315	92.5
14.75	1.324	90.6
14.85	1.332	91.1
14.94	1.341	91.6
15.04	1.350	90.4
15.14	1.359	89.3
15.24	1.367	91.7
15.34	1.376	92.7
15.44	1.385	92.2
15.54	1.394	93.7
15.64	1.403	93.1
15.74	1.412	92.2
15.84	1.421	92.7
15.94	1.430	93.1
16.04	1.439	90.4
16.18	1.452	91.3
16.26	1.459	93.6
16.36	1.468	91.4
16.44	1.475	93.5
16.54	1.484	93.1
16.64	1.493	92.9
16.74	1.502	94.0
16.84	1.511	93.2
16.94	1.520	94.4
17.04	1.529	94.7
17.14	1.538	93.6
17.24	1.547	96.4
17.34	1.556	91.6
17.44	1.565	94.6
17.54	1.574	92.2
17.67	1.586	91.0
17.76	1.594	89.1
17.86	1.603	89.6
17.94	1.610	87.4
18.04	1.619	89.5
18.14	1.628	89.9
18.24	1.637	90.1
18.34	1.646	91.2
18.44	1.655	91.5
18.54	1.665	92.5
18.64	1.678	89.9
18.74	1.691	91.1
18.84	1.704	92.3
18.94	1.717	91.8
19.04	1.729	90.8
19.12	1.740	92.1
19.22	1.753	94.5
19.34	1.768	91.6
19.44	1.781	93.8
19.54	1.794	93.4
19.64	1.807	93.8
19.74	1.819	93.9
19.84	1.832	94.9
19.94	1.845	92.8
20.04	1.858	93.6
20.14	1.871	89.5
20.24	1.884	92.6
20.34	1.897	92.3
20.44	1.909	92.6
20.54	1.922	92.6
20.64	1.935	92.8
20.72	1.945	89.7
20.81	1.957	89.0
20.94	1.974	88.1
21.04	1.987	89.7
21.14	1.999	90.0
21.24	2.012	87.0
21.34	2.025	91.5
21.44	2.038	90.8
21.54	2.051	91.7
21.66	2.066	91.1
21.74	2.077	95.4
21.84	2.089	94.2
21.97	2.106	92.7
22.07	2.119	93.3
22.15	2.129	92.5
22.24	2.141	91.3
22.34	2.154	92.2
22.44	2.167	89.5
22.54	2.179	90.8
22.64	2.192	89.6
22.74	2.205	89.3
22.84	2.218	89.8
22.94	2.231	89.1
23.02	2.241	88.9
23.14	2.257	88.2
23.24	2.269	90.8
23.34	2.282	90.3
23.44	2.295	90.8
23.54	2.308	91.9
23.64	2.321	91.0
23.74	2.334	90.2
23.84	2.347	91.4
23.94	2.359	89.5
24.04	2.372	90.4
24.13	2.384	88.2
24.25	2.399	91.6
24.36	2.413	91.0
24.46	2.426	90.2
24.56	2.439	92.4
24.64	2.449	91.0
24.74	2.462	92.9
24.84	2.474	91.2
24.94	2.484	89.7
25.04	2.495	91.8
25.14	2.505	91.8
25.24	2.515	92.1
25.34	2.526	90.9
27.94	2.793	91.3
28.04	2.804	88.7
28.14	2.814	89.0
28.22	2.822	91.3
28.32	2.832	92.9
28.44	2.845	91.5
28.54	2.855	92.6
28.63	2.864	93.8
28.75	2.877	90.9
28.86	2.888	91.8
28.95	2.897	91.1
29.05	2.908	92.2
29.14	2.917	92.7
29.34	2.937	91.8
29.44	2.948	95.0
29.54	2.958	92.2
29.64	2.968	92.4
29.74	2.979	91.3
29.84	2.989	90.9
29.94	3.000	94.0
30.04	3.010	90.9
30.13	3.020	92.5
30.24	3.031	91.1
30.36	3.044	92.0
30.44	3.052	91.4
30.54	3.063	90.6
30.64	3.073	93.0
30.74	3.084	90.1
30.84	3.095	88.2
30.94	3.105	89.1
31.04	3.116	87.2
31.14	3.126	89.6
31.22	3.135	91.0
31.32	3.145	90.6
31.44	3.158	90.1
31.54	3.168	88.3
31.63	3.178	90.8
31.74	3.190	90.4
31.86	3.202	90.4
31.96	3.213	91.3
32.05	3.222	91.9
32.14	3.232	93.4
32.24	3.242	92.2
32.34	3.253	91.4
32.44	3.263	91.5
32.54	3.274	91.9
32.64	3.285	92.5
32.74	3.295	90.4
32.85	3.307	89.0
32.86	3.308	91.0
32.94	3.316	91.8
33.04	3.327	95.3
33.14	3.337	91.1
33.24	3.348	92.2
33.34	3.358	92.4
33.44	3.369	92.7
33.54	3.380	90.6
33.64	3.390	93.2
33.74	3.401	91.6
33.83	3.410	91.1
33.92	3.420	93.3
34.04	3.432	92.6
34.14	3.443	88.7
34.24	3.453	89.6
34.34	3.464	89.7
34.44	3.475	91.2
34.54	3.485	90.7
34.64	3.496	89.7
34.74	3.506	92.1
34.84	3.517	91.0
34.94	3.527	87.3
35.04	3.538	88.1
35.14	3.548	90.2
35.24	3.559	87.3
35.34	3.570	86.9
35.43	3.579	86.6
35.54	3.591	87.2
35.64	3.601	88.4
35.74	3.612	88.4
35.94	3.633	89.2
36.04	3.643	91.0
36.14	3.654	90.5
36.24	3.665	86.9
36.34	3.675	90.2
36.44	3.686	88.0
36.54	3.696	89.6
36.64	3.707	89.3
36.74	3.717	89.3
36.84	3.728	91.1
36.94	3.738	90.5
37.04	3.749	92.0
37.14	3.760	90.7
37.24	3.770	89.7
115-710A-3H-		
19.21	2.317	77.7
19.26	2.325	80.0
19.31	2.334	85.6
19.36	2.342	76.1
19.41	2.351	81.1
19.46	2.360	83.2
19.52	2.370	73.8
19.58	2.380	84.2
19.61	2.386	86.4
19.66	2.394	86.1
19.71	2.403	75.0
19.76	2.411	81.6
19.81	2.420	83.1
19.86	2.429	78.8
19.91	2.437	72.7
19.96	2.446	66.8
20.01	2.454	68.7
20.06	2.463	60.7
20.11	2.471	69.8
20.16	2.475	71.5
20.21	2.479	76.5
20.27	2.485	73.9
20.31	2.488	69.3
20.37	2.493	77.1
20.40	2.496	78.6
20.46	2.501	82.3
20.51	2.505	82.6
20.56	2.509	69.3
20.61	2.514	83.7
20.66	2.518	67.4
20.71	2.522	71.1
20.76	2.527	75.9
20.81	2.531	78.0
20.86	2.535	80.2
20.91	2.539	78.9
20.96	2.544	64.0
21.02	2.549	65.8
21.08	2.554	74.7
21.11	2.557	64.3
21.16	2.561	75.4
21.21	2.565	81.5
21.26	2.569	81.0
21.31	2.574	84.1
21.36	2.578	76.0
21.41	2.582	82.5
21.46	2.587	82.0
21.51	2.591	82.9
21.56	2.595	81.0
21.61	2.599	73.5
21.66	2.604	70.1
21.71	2.608	67.1
21.77	2.613	75.3
21.81	2.617	75.5
21.87	2.622	77.1
21.90	2.624	80.6
22.21	2.651	69.1
22.26	2.655	79.3
22.31	2.659	77.1
22.36	2.664	75.5
22.41	2.668	74.7
22.46	2.672	75.7
22.52	2.677	65.9
22.58	2.683	65.3
22.61	2.685	69.4

Appendix (continued).

Depth (msbf)	Age (Ma)	$CaCO_3$ (%)
115-710A-3H- (Cont.)		
22.66	2.689	85.0
22.71	2.694	63.3
22.76	2.698	68.1
22.81	2.702	67.9
22.86	2.707	75.7
22.91	2.711	76.9
22.96	2.715	81.6
23.01	2.719	84.0
23.06	2.724	75.2
23.11	2.728	72.0
23.16	2.732	72.6
23.21	2.737	68.8
23.27	2.742	71.3
23.31	2.745	69.6
23.37	2.750	59.6
23.40	2.753	63.8
23.46	2.758	64.4
23.51	2.762	71.0
23.56	2.767	77.6
23.61	2.771	73.9
23.66	2.775	67.8
115-710A-4H-		
28.81	3.887	73.7
28.86	3.891	67.8
28.91	3.895	73.9
28.96	3.899	78.0
29.01	3.902	72.9
29.06	3.906	69.2
29.12	3.911	72.8
29.17	3.915	76.3
29.21	3.918	72.2
29.26	3.921	68.4
29.31	3.925	68.5
29.36	3.929	64.6
29.41	3.933	68.7
29.46	3.937	55.9
29.52	3.941	63.0
29.56	3.944	69.8
29.61	3.948	64.8
29.66	3.952	64.1
29.71	3.956	70.0
29.76	3.959	69.3
29.81	3.963	69.5
29.87	3.968	72.5
29.91	3.971	60.6
29.97	3.975	68.8
30.02	3.979	65.3
30.06	3.982	77.5
30.12	3.987	69.4
30.17	3.991	69.5
30.21	3.994	70.4
30.26	3.997	67.3
30.31	4.001	74.1
30.36	4.005	74.1
30.41	4.009	77.7
30.46	4.013	71.6
30.51	4.016	71.3
30.56	4.020	69.5
30.62	4.025	70.2
30.67	4.028	69.7
30.71	4.032	76.1
30.77	4.036	79.0
30.81	4.039	78.9
30.86	4.043	70.3
30.91	4.047	71.6
30.96	4.051	67.9
31.02	4.055	86.2
31.06	4.058	65.8
31.11	4.062	71.2
31.16	4.066	77.8
31.21	4.069	67.9
31.26	4.073	69.6
31.31	4.077	72.7
31.37	4.082	71.0

Depth (msbf)	Age (Ma)	$CaCO_3$ (%)
115-710A-4H- (Cont.)		
31.41	4.085	68.7
31.47	4.089	69.3
31.52	4.093	76.2
31.56	4.096	76.6
31.62	4.101	78.8
31.67	4.104	78.4
31.71	4.107	78.2
31.76	4.111	75.7
31.81	4.115	63.4
31.86	4.119	68.1
31.96	4.126	54.8
32.01	4.130	56.5
32.06	4.134	55.0
32.12	4.139	47.2
32.17	4.142	56.4
32.21	4.145	64.3
32.26	4.149	58.4
32.31	4.153	60.4
32.36	4.157	59.3
32.41	4.161	58.7
32.46	4.164	49.8
32.52	4.169	66.5
32.56	4.172	59.3
32.61	4.176	58.9
32.66	4.180	70.4
32.71	4.183	65.4
32.76	4.187	67.4
32.81	4.191	69.7
32.87	4.196	73.9
32.91	4.199	72.4
32.97	4.203	70.9
33.02	4.207	71.8
33.06	4.210	76.0
33.12	4.215	76.0
33.17	4.218	74.9
33.21	4.221	67.5
33.26	4.225	77.1
33.31	4.229	76.3
33.36	4.233	80.8
33.41	4.237	77.7
33.46	4.240	75.4
33.51	4.244	60.7
33.56	4.248	71.1
33.62	4.253	73.7
33.67	4.256	66.5
33.71	4.259	69.1
33.76	4.263	69.2
33.81	4.267	69.2
33.86	4.271	66.5
33.91	4.275	76.4
33.96	4.278	61.3
34.02	4.283	68.0
34.06	4.286	70.3
34.11	4.290	62.3
34.16	4.294	73.3
34.21	4.297	68.5
34.26	4.301	70.2
34.31	4.305	73.0
34.37	4.309	74.6
34.41	4.313	75.6
34.47	4.317	67.9
34.52	4.321	63.1
34.56	4.324	81.4
34.62	4.328	79.4
34.67	4.332	80.8
34.71	4.335	72.7
34.75	4.338	65.4
34.81	4.343	67.2
34.86	4.347	75.7
34.91	4.351	78.4
34.96	4.354	77.1
35.01	4.358	75.5
35.06	4.362	76.5
35.12	4.366	75.1
35.17	4.370	70.0
35.21	4.373	66.0

Depth (msbf)	Age (Ma)	$CaCO_3$ (%)
115-710A-4H- (Cont.)		
35.26	4.377	69.2
35.31	4.381	77.2
35.36	4.385	80.0
35.41	4.388	78.8
35.46	4.392	78.8
35.52	4.397	78.0
35.56	4.400	73.4
35.61	4.404	78.5
35.66	4.407	69.5
35.71	4.411	67.4
35.76	4.415	75.9
35.81	4.419	78.0
35.87	4.423	75.7
35.91	4.426	79.3
35.97	4.431	81.2
36.02	4.435	78.4
36.06	4.438	81.8
36.12	4.442	76.0
36.17	4.446	70.7
36.21	4.449	74.4
36.26	4.453	72.6
36.31	4.457	81.3
36.36	4.461	80.5
36.41	4.464	69.2
36.46	4.468	74.5
36.51	4.472	68.0
36.56	4.476	62.6
36.62	4.480	76.9
36.67	4.484	76.0
36.71	4.487	78.7
36.76	4.491	79.7
36.81	4.495	78.2
36.86	4.499	82.0
36.91	4.502	75.9
36.96	4.506	77.8
37.02	4.511	58.4
37.06	4.514	70.4
37.11	4.518	68.1
37.16	4.521	66.5
37.21	4.525	75.3
37.26	4.529	62.0
37.31	4.533	75.4
37.36	4.537	72.2
37.41	4.540	79.1
37.47	4.545	79.4
37.52	4.549	77.4
37.56	4.552	73.1
37.62	4.556	69.4
37.67	4.560	73.0
37.71	4.563	73.2
37.76	4.567	66.4
37.81	4.571	83.1
37.86	4.575	82.0
37.91	4.578	78.2
37.96	4.582	81.7
38.01	4.586	72.2
38.06	4.590	77.6
38.12	4.594	80.7
38.17	4.598	80.1
38.21	4.601	76.7
38.26	4.605	74.9
38.31	4.609	71.7
38.36	4.613	83.0
115-710B-4H-		
25.81	2.938	73.4
25.86	2.952	63.3
25.91	2.966	66.9
25.96	2.979	66.0
26.01	2.993	64.2
26.06	3.006	60.9
26.10	3.017	60.4
26.16	3.033	58.8
26.21	3.047	61.6
26.26	3.061	59.3

Depth (msbf)	Age (Ma)	$CaCO_3$ (%)
115-710B-4H- (Cont.)		
26.31	3.074	68.1
26.36	3.088	69.5
26.41	3.101	74.0
26.46	3.115	74.9
26.50	3.126	67.9
26.56	3.142	59.5
26.61	3.156	63.8
26.66	3.169	66.9
26.71	3.181	59.4
26.76	3.188	70.1
26.82	3.196	70.9
26.86	3.202	73.0
26.91	3.209	74.2
26.96	3.216	75.3
27.01	3.223	71.9
27.06	3.230	72.6
27.11	3.236	71.1
27.16	3.243	75.3
27.21	3.250	72.2
27.26	3.257	68.0
27.31	3.264	58.7
27.36	3.271	62.2
27.41	3.278	60.8
27.46	3.284	69.3
27.51	3.291	59.5
27.56	3.298	63.3
27.60	3.304	65.4
27.66	3.312	62.4
27.71	3.319	71.1
27.76	3.326	70.1
27.81	3.333	64.4
27.86	3.340	65.9
27.91	3.346	68.7
27.96	3.353	70.6
28.01	3.360	58.9
28.06	3.367	63.2
28.11	3.374	63.1
28.16	3.381	65.4
28.21	3.388	62.3
28.26	3.395	70.8
28.31	3.401	70.8
28.36	3.408	74.1
28.41	3.414	70.8
28.46	3.421	74.9
28.51	3.427	71.4
28.56	3.434	73.0
28.62	3.442	70.9
28.66	3.447	68.2
28.71	3.453	71.3
28.76	3.460	69.9
28.81	3.466	61.8
28.86	3.473	58.0
28.91	3.479	67.2
28.96	3.486	77.9
29.01	3.492	73.6
29.06	3.499	72.8
29.10	3.504	64.6
29.16	3.512	59.5
29.21	3.518	58.0
29.26	3.525	68.5
29.31	3.531	63.6
29.36	3.538	63.9
29.41	3.544	67.6
29.46	3.550	68.4
29.50	3.556	68.2
29.56	3.563	69.5
29.61	3.570	71.1
29.66	3.576	72.9
29.71	3.583	73.1
29.76	3.589	69.4
29.81	3.596	64.1
29.86	3.602	64.6
29.91	3.609	62.4
29.96	3.615	57.1
30.01	3.622	68.0
30.06	3.628	62.7

Depth (msbf)	Age (Ma)	$CaCO_3$ (%)
115-710B-4H- (Cont.)		
30.12	3.636	62.4
30.16	3.641	64.5
30.21	3.648	53.8
30.26	3.654	69.9
30.31	3.661	69.5
30.36	3.667	68.1
30.41	3.674	61.8
30.46	3.680	68.7
30.51	3.687	70.5
30.56	3.693	65.5
30.60	3.698	64.4
30.66	3.706	71.6
30.71	3.713	66.5
30.76	3.719	66.3
30.81	3.726	62.1
30.86	3.732	66.8
30.91	3.739	58.3
30.96	3.745	61.4
31.00	3.750	60.2
31.06	3.758	56.3
31.11	3.765	64.3
31.16	3.771	69.8
31.21	3.778	67.7
31.26	3.784	70.0
31.31	3.790	68.6
31.36	3.797	71.3
31.41	3.803	73.3
31.46	3.810	74.6
31.51	3.816	73.5
31.56	3.823	73.2
31.62	3.831	74.8
31.66	3.836	75.4
31.71	3.842	76.4
31.76	3.849	73.1
31.81	3.855	75.8
31.86	3.862	76.4
31.91	3.868	79.1
31.96	3.875	77.4
32.01	3.881	76.1
32.06	3.885	80.6
32.10	3.888	79.1
32.16	3.893	78.9
32.21	3.897	76.7
32.26	3.901	76.4
32.31	3.905	76.5
32.36	3.909	73.8
32.41	3.914	73.9
32.46	3.918	70.2
32.50	3.921	67.9
32.56	3.926	67.8
32.61	3.930	69.1
32.66	3.934	70.9
32.71	3.938	70.7
32.76	3.942	71.2
32.81	3.946	70.9
32.86	3.950	72.1
32.91	3.954	72.1
32.96	3.959	69.3
33.01	3.963	68.2
33.06	3.967	69.8
115-710B-5H-		
38.11	4.557	82.1
38.16	4.561	82.2
38.21	4.565	81.1
38.26	4.569	83.0
38.31	4.573	83.4
38.36	4.578	81.9
38.41	4.582	83.6
38.46	4.586	77.6
38.51	4.590	79.9
38.56	4.594	84.7
38.61	4.598	85.3
38.66	4.602	85.9
38.71	4.606	82.7

Appendix (continued).

Depth (msbf)	Age (Ma)	$CaCO_3$ (%)
115-710B-5H- (Cont.)		
38.76	4.610	83.3
38.81	4.615	83.2
38.86	4.619	84.8
38.91	4.623	81.1
38.96	4.627	75.7
39.01	4.631	79.3
39.06	4.635	83.0
39.11	4.639	80.3
39.16	4.643	77.9
39.21	4.647	79.2
39.26	4.652	79.9
39.31	4.656	76.3
39.36	4.660	76.3
39.41	4.664	76.1
39.46	4.668	77.3
39.51	4.672	79.9
39.56	4.676	79.8
39.61	4.680	79.3
39.66	4.684	76.3
39.71	4.689	80.7
39.76	4.693	82.5
39.81	4.697	84.4
39.86	4.701	82.3
39.89	4.703	77.4
39.91	4.705	75.4
39.96	4.709	76.2
40.01	4.713	76.2
40.06	4.717	73.1
40.11	4.721	71.9
40.16	4.726	76.8
40.21	4.730	79.8
40.26	4.734	79.3
40.31	4.738	76.8
40.36	4.742	77.2
40.41	4.746	78.7
40.47	4.751	79.3
40.51	4.754	78.9
40.58	4.760	72.9
40.61	4.763	75.9
40.66	4.767	75.5
40.71	4.771	78.6
40.76	4.775	78.2
115-711A-2H-		
8.20	1.380	14.8
8.25	1.389	30.8
8.30	1.398	32.7
8.35	1.406	34.0
8.40	1.415	24.8
8.46	1.426	28.1
8.51	1.434	39.4
8.56	1.443	47.0
8.61	1.452	35.3
8.65	1.459	29.9
8.69	1.466	37.2
8.75	1.476	47.5
8.80	1.485	59.2
8.85	1.494	82.6
8.90	1.502	73.5
8.95	1.511	62.8
9.00	1.520	56.1
9.05	1.529	67.1
9.10	1.538	63.3
9.15	1.546	58.1
9.21	1.557	34.7
9.30	1.572	44.4
9.35	1.581	77.3
9.40	1.590	73.2
9.50	1.607	43.8
9.65	1.634	21.4
9.70	1.642	34.8
9.75	1.651	39.8
9.80	1.660	35.4
9.84	1.672	31.0
9.90	1.690	35.4

Depth (msbf)	Age (Ma)	$CaCO_3$ (%)
115-711A-2H- (Cont.)		
9.96	1.707	38.3
10.00	1.719	48.9
10.05	1.734	55.1
10.10	1.749	36.4
10.16	1.767	34.3
10.20	1.778	34.6
10.26	1.796	45.0
10.30	1.808	24.7
10.36	1.826	32.5
10.45	1.853	29.5
10.50	1.867	22.9
10.55	1.882	30.4
10.63	1.906	43.5
10.72	1.932	32.5
10.77	1.947	46.7
10.81	1.959	44.2
10.86	1.974	54.5
10.91	1.989	44.4
10.95	2.001	35.1
11.01	2.018	31.2
11.06	2.033	40.6
11.15	2.060	33.8
11.20	2.075	43.2
11.25	2.089	38.9
11.30	2.104	33.8
11.35	2.119	39.4
11.39	2.131	28.5
11.46	2.152	40.3
11.50	2.164	30.3
11.55	2.178	40.5
11.61	2.196	38.0
11.65	2.208	32.1
11.70	2.223	41.8
11.75	2.238	26.9
11.80	2.252	34.4
11.85	2.267	50.3
11.89	2.279	28.5
11.91	2.285	24.0
11.95	2.297	53.5
12.05	2.326	41.5
12.21	2.374	15.8
12.27	2.392	9.8
12.36	2.418	13.4
12.41	2.433	19.5
12.45	2.445	22.7
12.51	2.463	22.4
12.66	2.507	28.4
12.71	2.522	26.7
12.76	2.537	27.3
12.81	2.552	28.5
12.86	2.566	28.2
12.90	2.578	28.1
12.98	2.602	18.0
115-711A-3H-		
18.10	4.118	12.6
18.15	4.133	11.7
18.21	4.151	7.4
18.25	4.163	9.3
18.30	4.178	7.4
18.40	4.207	1.6
18.44	4.219	5.0
18.50	4.237	3.1
18.55	4.252	8.8
18.59	4.264	4.0
18.66	4.284	6.7
18.70	4.296	5.4
18.80	4.326	5.5
18.84	4.338	3.4
18.90	4.355	4.3
18.95	4.370	3.8
19.00	4.385	3.0
19.05	4.400	4.9
19.10	4.415	7.5
19.15	4.429	10.8

Depth (msbf)	Age (Ma)	$CaCO_3$ (%)
115-711A-3H- (Cont.)		
19.20	4.444	12.8
19.25	4.459	15.3
19.30	4.474	15.3
19.35	4.489	18.1
19.40	4.503	14.9
19.45	4.518	13.7
19.50	4.533	13.9
19.55	4.548	16.2
19.60	4.563	23.7
19.65	4.577	21.0
19.70	4.592	12.0
19.75	4.607	12.6
19.80	4.622	25.0
19.85	4.637	15.9
19.90	4.652	14.6
19.95	4.666	16.1
20.00	4.681	13.4
20.05	4.696	12.6
20.10	4.711	9.6
20.15	4.726	9.6
20.22	4.746	8.2
20.25	4.755	7.8
20.30	4.770	9.0
20.34	4.782	7.5
20.40	4.800	8.3
20.45	4.814	7.1
20.50	4.829	10.2
20.55	4.844	7.0
20.60	4.859	5.5
20.65	4.874	6.9
20.70	4.888	6.7
115-711B-3H-		
11.75	2.427	26.4
11.80	2.441	17.5
11.85	2.456	19.6
11.90	2.470	13.7
11.95	2.487	22.1
12.00	2.504	21.5
12.05	2.522	10.8
12.10	2.539	15.6
12.15	2.556	27.8
12.20	2.573	31.3
12.25	2.591	30.4
12.30	2.608	28.4
12.35	2.625	19.4
12.40	2.642	15.8
12.45	2.659	22.0
12.50	2.677	15.9
12.55	2.694	15.2
12.60	2.711	12.8
12.65	2.728	11.2
12.70	2.746	17.8
12.75	2.763	29.2
12.80	2.780	30.1
12.85	2.797	11.8
12.90	2.814	11.1
12.95	2.832	9.0
13.00	2.849	8.8
13.05	2.866	9.0
13.10	2.883	7.5
13.15	2.901	7.1
13.20	2.918	5.7
13.25	2.935	8.5
13.30	2.952	8.0
13.35	2.969	6.3
13.40	2.987	3.6
13.45	3.004	5.3
13.50	3.021	4.3
13.55	3.038	2.1
13.60	3.056	1.7
13.65	3.073	4.9
13.71	3.093	2.9
13.75	3.107	2.0
13.80	3.124	1.8

Depth (msbf)	Age (Ma)	$CaCO_3$ (%)
115-711B-3H- (Cont.)		
13.85	3.142	2.0
13.90	3.159	2.9
13.95	3.176	2.9
14.01	3.197	5.1
14.05	3.211	4.4
14.10	3.228	2.1
14.15	3.245	3.9
14.20	3.262	1.2
14.25	3.279	0.7
14.30	3.297	1.2
14.34	3.310	2.8
14.40	3.331	2.7
14.45	3.348	3.1
14.50	3.366	3.2
14.55	3.383	3.0
14.60	3.400	2.2
14.65	3.414	4.1
14.70	3.429	3.7
14.75	3.443	1.1
14.80	3.457	0.8
14.85	3.471	0.8
14.90	3.486	0.7
14.95	3.500	0.8
15.00	3.514	0.9
15.05	3.528	0.6
15.10	3.543	0.6
15.15	3.557	0.7
15.20	3.571	0.5
15.25	3.585	0.6
15.30	3.600	0.4
15.35	3.614	0.5
15.40	3.628	0.4
15.45	3.643	0.4
15.50	3.657	0.4
15.55	3.671	0.4
15.60	3.685	0.6
15.65	3.700	0.5
15.70	3.714	0.5
15.75	3.728	0.5
15.80	3.742	0.4
15.85	3.757	0.3
15.90	3.771	0.3
15.95	3.785	0.4
16.00	3.800	0.5
16.05	3.814	0.6
16.10	3.828	0.6
16.15	3.842	0.8
16.20	3.857	0.5
16.25	3.871	0.6
16.30	3.885	0.8
16.35	3.899	0.5
16.40	3.914	0.5
16.45	3.928	0.9
16.50	3.942	1.0
16.55	3.956	0.5
16.60	3.971	1.0
16.65	3.985	0.8
16.70	3.999	1.2
16.75	4.014	0.8
16.80	4.028	1.8
16.85	4.042	1.9
16.90	4.056	0.5
16.95	4.071	0.5
17.00	4.085	1.1
17.05	4.099	1.0
17.10	4.113	1.1
17.15	4.128	0.8
17.20	4.142	0.6
17.25	4.156	0.4
17.30	4.170	0.4
17.35	4.185	0.7
17.40	4.199	1.2
17.45	4.213	1.2
17.50	4.228	1.2
17.55	4.242	1.2
17.60	4.256	1.5

Depth (msbf)	Age (Ma)	$CaCO_3$ (%)
115-711B-3H- (Cont.)		
17.65	4.270	0.4
17.70	4.285	0.8
17.75	4.299	2.5
17.80	4.313	2.7
17.85	4.327	1.9
17.90	4.342	1.7
17.95	4.356	1.4
18.00	4.370	2.4
18.05	4.385	2.1
18.10	4.399	1.9
18.15	4.413	4.3
18.20	4.427	6.3
18.25	4.442	2.4
18.30	4.456	3.1
18.35	4.470	6.0
18.40	4.484	6.2
18.45	4.499	7.9
18.50	4.513	9.1
18.55	4.527	16.6
18.60	4.541	18.6
18.65	4.556	22.5
18.70	4.570	23.9
18.75	4.584	12.8
18.80	4.599	14.8
18.85	4.613	15.3
18.90	4.627	15.8
18.95	4.641	17.6
19.00	4.656	14.1
19.05	4.670	14.0
19.10	4.684	7.4
19.15	4.698	7.7
19.20	4.713	6.9